MAUSAM, **76**, 4 (October 2025), 1047-1062

MAUSAM

DOI: https://doi.org/10.54302/mausam.v76i4.7103
Homepage: https://mausamjournal.imd.gov.in/index.php/MAUSAM

UDC No.551.515.2:502.3(267.64)

Assessing aerosol interactions and re-distribution during very severe cyclonic storm 'Vardah' in the Bay of Bengal

VIVEK SINGH[1]*, HITESH GUPTA[2#^], ARUN KUMAR[3&], AMARENDRA SINGH[3$], SUMIT SINGH[4], BHAGYALAXMI VERMA[5!], CHARU JHAMARIA[5@], GAURAV TIWARI[6], ASHISH ROUTRAY[7], DILEEP KUMAR GUPTA[8], ABHISHEK LODH[9], and ARPAN BHATTACHARJEE[2]

[1] *Indian Institute of Tropical Meteorology (Delhi Branch), Prof Ramnath Vij Marg, MoES, New Delhi, 110060, India*

[2] *School of Earth, Ocean and Climate Sciences, Indian Institute of Technology Bhubaneswar, Odisha, 752050, India (^a24ao09013@iitbbs.ac.in)*

[3] *Centre for Atmospheric Sciences, Indian Institute of Technology Delhi, Hauz Khas, New Delhi, 110016, India (&aruniitbbs@gmail.com, $amar.singh712@gmail.com)*

[4] *Civil Engineering Department, Institute of Engineering and Technology (IET), Lucknow, U.P. 226021, India (sumitvedsingh@gmail.com)*

[5] *Department of Environmental Science, IIS (Deemed to be University), Jaipur, India (!vermabhagya94@gmail.com, @charu.jhamaria@iisuniv.ac.in)*

[6] *Center for Environmental Remote Sensing, Chiba University, Japan (gtiwari506@gmail.com)*

[7] *National Centre for Medium Range Weather Forecasting, A-50, Sector-62, NOIDA, MoES, Government of India (ashishroutray.iitd@gmail.com)*

[8] *Department of Electronics, Galgotias University, Greater NOIDA, UP (dileepgupta85@gmail.com)*

[9] *Swedish Meteorological and Hydrological Institute, Folkborgsvägen 17, Norrkoping, Sweden (abhishek.iitd.lodh@gmail.com)*

(*Received 09 May 2025, Accepted 05 September 2025*)

Corresponding author's email: *vivek.singh@tropmet.res.in, #hg13@iitbbs.ac.in

सार– वर्तमान अध्ययन बंगाल की खाड़ी (BoB) में एक अति प्रचण्ड चक्रवाती तूफान (VSCS) वरदा (6 से 13 दिसंबर, 2016) के दौरान पुनःविश्लेषण और उपग्रह प्रेक्षणों का उपयोग करते हुए वायुविलय की परस्पर क्रिया और पुनर्वितरण की जांच करता है। विस्तृत विश्लेषण उष्णकटिबंधीय चक्रवात (TC) प्रेरित वर्षा पर वायुविलय के प्रभावों पर केंद्रित है जिसमें वायुविलय लोडिंग की जांच, चक्रवात के पथ के दौरान उसके वितरण में परिवर्तन शामिल है। जैसे-जैसे चक्रवात वरदा एक प्रचण्ड चक्रवाती तूफान (एससीएस) से अति प्रचण्ड चक्रवाती तूफान में परिवर्तित हुआ वर्षा दर (पीआर) में क्रमिक कमी देखी गई, साथ ही निम्न क्षोभमंडलीय स्थिरता (LTS). में भी वृद्धि देखी गई। वायुविलय से समृद्ध उत्तर-पूर्वी हिमालयी क्षेत्र से चक्रवात की ओर आने वाली हवाओं के परिणामस्वरूप चक्रवात में वायुविलय का महत्वपूर्ण प्रवाह हुआ। उष्णकटिबंधीय चक्रवात वरदा के प्रचण्ड चक्रवाती तूफान और अति प्रचण्ड चक्रवाती तूफान के चरणों के दौरान क्रमशः मध्य और पश्चिमी बंगाल की खाड़ी में और भी अधिक वायुविलय लोडिंग दर्ज की गई। ऐसा संभवतः उत्तर-पूर्वी हिमालयी क्षेत्र से चक्रवात की ओर आने वाली तेज हवाओं के कारण हुआ होगा, क्योंकि यह तटीय क्षेत्र के निकट पहुंच रहा था। तीनों चरणों (अर्थात चक्रवाती तूफान, प्रचण्ड चक्रवाती तूफान और अति प्रचण्ड चक्रवाती तूफान) के दौरान वायुविलय के स्थानिक वितरण और वर्षा दर की जांच से पता चलता है कि चक्रवात वरदा के आने से पहले वायुविलय की उपस्थिति ने वर्षा को दबाने में महत्वपूर्ण भूमिका निभाई। इसके अतिरिक्त, AOD की स्थानिक-कालिक विसंगतियों में तीव्र विरोधाभास देखा गया, जिसमें मानवजनित वायुविलय तूफान के केंद्र के पास गीले अपमार्जन के कारण अवक्षणीय हो गए, जबकि समुद्री नमक जैसे प्राकृतिक वायुविलय में तूफान पथ के साथ बढोतरी हुई, जिससे चक्रवात की वायुविलय के सफाईकर्ता और पुनर्वितरक दोनों के रूप में दोहरी भूमिका पर प्रकाश पड़ा। इसके अलावा, हमारे विश्लेषण से पता चला कि चक्रवाती तूफान वरदा ने समुद्र से लाकर चेन्नई के ऊपर काफी मात्रा में वायुविलय जमा कर दिया। ये परिणाम वायुविलय के पुनर्वितरण और बंगाल की खाड़ी पर चक्रवातों द्वारा प्रेरित वर्षा पर उनके प्रभाव को समझने में महत्वपूर्ण योगदान देते हैं।

ABSTRACT: Utilizing reanalysis and satellite observations, the present study investigates the interactions and redistribution of aerosols during a Very Severe Cyclonic Storm (VSCS) Vardah (6-13 December, 2016) in the Bay of Bengal (BoB). The detailed analysis focuses on the effects of aerosols on the tropical cyclone (TC) induced precipitation, including an examination of aerosol loading, changes in their distribution during the passage of the cyclone. As cyclone Vardah matured from a Severe Cyclonic Storm (SCS) to VSCS, a gradual reduction in the Precipitation Rate (PR) was observed, accompanied by an increasing trend of Lower Tropospheric Stability (LTS). Winds originating from the north-eastern Himalayan region and transporting aerosols from the aerosol-rich Indo-Gangetic Plain (IGP) carried a substantial amount of aerosol particles toward the cyclone, resulting in a significant influx into its circulation. Even more aerosol loading was recorded over the central and western BoB during the SCS and VSCS stages of TC Vardah, respectively. This could be due to the strong drag of winds from the north-eastern Himalayan region towards the cyclone as it approached the coastal region. Investigation of the spatial distribution of aerosols and precipitation rate during all three stages (i.e., Cyclonic Storm (CS), SCS, and VSCS) revealed that the presence of aerosols played a significant role in suppressing precipitation before cyclone Vardah made landfall. Additionally, spatio-temporal anomalies of AOD showed a sharp contrast, with anthropogenic aerosols depleted near the storm core due to wet scavenging, while natural aerosols such as sea salt were enhanced along the storm track, highlighting the cyclone's dual role as both a cleanser and redistributor of aerosols. Further, our analysis revealed that TC Vardah deposited a significant amount of aerosols over Chennai, bringing it from the ocean. These results make an important contribution to understanding the redistribution of aerosols and their impact on precipitation induced by cyclones over the BoB.

Key words–Bay of Bengal, Tropical cyclone, Precipitation rate, Lower tropospheric stability, Aerosol optical depth.

1. Introduction

TCs are among the most destructive synoptic weather systems, posing significant threats to coastal regions of the North Indian Ocean (NIO), particularly the BoB (Tiwari *et al.,* 2022; Tiwari *et al.,* 2022). TCs in the NIO account for about 6-7% of global cyclone occurrences but result in 80% of global cyclone-induced casualties, emphasizing the severity of their impact in this region (Singh *et al.,* 2023; Rajasree *et al.,* 2016). One of the critical factors contributing to this high casualty rate is the rapid intensification (RI) of cyclones before landfall (Hendricks *et al.,* 2019; Singh *et al.,* 2022, Garner, 2023). The BoB has experienced increasing cyclone intensification rates over the past few decades, driven by significant changes in upper ocean conditions like surface and subsurface marine heat waves, and significantly influencing the biophysical response of the ocean (Mandal *et al.,* 2018; Busireddy *et al.,* 2019, Balaguru *et al.,* 2022, Cheriyan *et al.,* 2022, Rathore *et al.,* 2022, Gupta *et al.,* 2024, Sengupta *et al.,* 2008, Gramer *et al.,* 2022, Gupta *et al.,* 2025, Sil *et al.,* 2021, Singh and Roxy, 2022; Yamada *et al.,* 2010). Further, the impact of aerosols on cyclone formation and intensification has garnered significant attention in recent years (Pravia-Sarabia *et al.,* 2021; Zhang *et al.,* 2021; Zhao *et al.,* 2020).

The BoB region, heavily polluted by emissions, receives aerosols from both natural sources, such as sea spray and dust storms, and anthropogenic sources, including industrial activities and biomass burning (Kumari *et al.,* 2022; Kumari *et al.,* 2022; Sarkar *et al.,* 2021; Yadav *et al.,* 2021, Kumar and Tiwari, 2023). These aerosols interact with various components of the coupled ocean-atmosphere system, including the ocean surface, the atmospheric boundary layer (ABL), along with upper-level outflow layer of cyclones (Betsy *et al.,* 2024; Kompalli *et al.,* 2021, Ventura *et al.,* 2021). These interactions can significantly alter the intensity and structure of TCs (Wadler *et al.,* 2023).

Aerosols influence sea surface temperature (SST), which is crucial parameter for cyclogenesis and cyclone intensification, and affect the thermodynamic conditions necessary for these processes (Diao *et al.,* 2021, Murakami, 2022, Zhang *et al.,* 2023). Studies have demonstrated that aerosols can impact the precipitation formation process, precipitation redistribution, and TC intensities through radiative and microphysical mechanisms (Luo *et al.,* 2019, Panda *et al.,* 2023, Zhao *et al.,* 2018). In particular, the radiative impacts of aerosols have been identified as a key factor influencing long-term temperature variations in the NIO (Chiacchio *et al.,* 2017). The dual role of aerosols in enhancing and suppressing TC intensity through radiative and microphysical mechanisms, respectively, has also been well-documented (Yang *et al.,* 2018; Evan *et al.,* 2011; Cotton *et al.,* 2012; Zhang and Zhou, 2021; Reale *et al.,* 2014, Herbener *et al.,* 2014, Lin *et al.,* 2023, Wang *et al.,* 2014). Despite extensive research worldwide, the precise contribution of aerosols to TC-induced precipitation and aerosol re-distribution remains unclear over the Indian region (Nair *et al.,* 2020). So, understanding the interactions between aerosols and TCs is crucial for improving cyclone prediction and assessing the broader climate impacts of these systems. The present study aims to assess the contribution of aerosols to TC-induced precipitation over the BoB, focusing on the interactions and redistribution of aerosols during the VSCS 'Vardah' (2016). The VSCS developed over the warm waters of the BoB between 6 and 13 December 2016, making landfall near 'Chennai' between 0930 and 1130 UTC on 12 December 2016. Chennai, a major metropolitan city of India, remains

relatively less explored with respect to cyclone-induced aerosol redistribution and interactions, thereby providing a suitable case study for cyclone–aerosol research. By analyzing AOD, Ångström Exponent (AE), sea-salt $PM_{2.5}$ and other aerosol parameters in conjunction with key atmospheric and oceanic variables, this study seeks to elucidate the complex interactions between aerosols & TCs. The data and methodology are presented in Section 2, the synoptic conditions in Section 3, followed by the results and discussion in Section 4 & the conclusions in Section 5.

2. Data and methodology

A range of space-borne satellite datasets and reanalysis data used in the present study are listed in Table 1, together with their temporal and spatial resolutions. Further, descriptions of the satellite observations, and reanalysis products are provided below.

2.1. *Satellite and reanalysis data products*

In the present study, we utilized reanalysis data from the European Centre for Medium-Range Weather Forecasting (ECMWF) version-5 (ERA-5) datasets. Our analysis incorporated six-hourly data of temperature, wind, relative humidity, relative vorticity, convective available potential energy (CAPE), and convective inhibition (CIN) across various pressure levels ranging from 1000 hPa to 100 hPa. The spatial resolution of data is approximately 12 km x 12 km (Dee *et al.*, 2011). Additionally, we utilized the daily National Oceanic and Atmospheric Administration (NOAA) Optimum Interpolation Sea Surface Temperature (OISST) dataset (available at 0.25°x 0.25° spatial resolution) to understand the spatial distribution of SST during various stages of the cyclone Vardah. The SST anomaly are calculated with respect to climatological period of 1993–2023.

2.2. *GPM and AOD datasets*

The Earth Observing System Data and Information System (EOSDIS) employs a grid-point statistical interpolation analysis system (Liu *et al.*, 2017) to organize and archive data products from the Global Precipitation Measurement (GPM) mission at the Goddard Earth Sciences Data and Information Services Center (GES DISC). EOSDIS categorizes GPM data into three distinct product levels to streamline data management and accessibility. For our study, we have utilized Tropical Rainfall Measuring Mission (TRMM) precipitation datasets, which provided data with a spatial grid resolution of 0.625° x 0.5° and a temporal resolution of 6 hours. Additionally, we have used AOD data products from the Moderate Resolution Imaging Spectroradiometer (MODIS) available at a spatial resolution of 0.625°x 0.5°.

TABLE 1

Spatial and temporal resolution of datasets

Data	Resolution (Spatial/Temporal)
Cyclone best-track data	3-Hourly
'u' & 'v' components of winds(m/s)	(Daily & monthly)/ (0.25°x 0.25°)
AOD (Unit less)	(Daily & monthly)/ (0.5°x 0.625°)
Relative vorticity (sec^{-1})	(Daily & monthly)/ (0.25°x 0.25°)
CAPE (J/Kg)	(Daily & monthly)/ (0.25°x 0.25°)
Potential temperature (K)	(Daily & monthly)/ (0.5°x 0.625°)
CIN(J/Kg)	(Daily & monthly)/ (0.25°x 0.25°)
Relative humidity (%)	(Daily & monthly)/ (0.25°x 0.25°)
Precipitation rate (mm/hr)	(Daily & monthly)/ (0.5°x 0.625°)
Sea surface temperature (°C)	(Daily) (0.25°x 0.25°)

2.3. *Data analysis procedures*

TC Vardah was a severe tropical cyclone that struck the southeastern coast of India in December 2016. It caused widespread damage in 'Chennai' and its surrounding areas, with high winds, heavy rainfall, and extensive flooding. The cyclone was notable for its RI and the significant impact on urban infrastructure (Bhavithra, & Sannasiraj; 2022). Due to this peculiar behavior, further, various atmospheric parameters of TC 'Vardah' were analyzed along the track to have an in-depth understanding of the cyclone behavior. Several dynamic parameters such as the Precipitation Rate (PR), wind speed, LTS, CAPE, and CIN were analyzed using 6-hourly data. These parameters were averaged within a moving box of size (1.5°x1.5°), with the cyclone's eye at its center. LTS was computed by subtracting the surface potential temperature from the potential temperature (**θ**) present at a level of 700 hPa.

(i.e., $LTS = \theta_{700} - \theta_{surf}$)

Pressure (P in hPa), gas constant (R with a value of 287.058 J/Kg/K), temperature (T in Kelvin), acceleration due to gravity (g), vertical velocities (W), can be used to obtain Omega (ω), which represents vertical velocity in pressure coordinate. It can be obtained through the formula: $-(P/RT) \times g \times W$. To examine the variation of AOD and Relative Humidity (RH) with wind flow direction at different vertical levels before, during, and after the cyclone, this study considers three distinct time periods: Pre-Cyclone (November 30th to December 5th, 2016), During Cyclone (December 6th to December 12th, 2016), and Post-Cyclone (December 13th to December 19th, 2016). To more thoroughly analyze the impact and redistribution of aerosols during Cyclone Vardah, the cyclonic period was divided into three distinct stages.

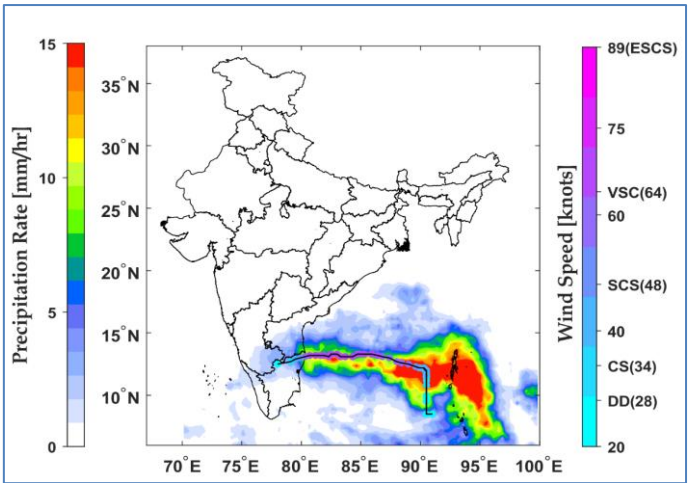

Fig. 1. The track of cyclone Vardah and the average precipitation rate from 6th to 12th December 2016. The dotted line illustrates the cyclone's track, while overlaid points indicate the different stages of cyclone Vardah. The background color represents the precipitation rate in mm/hr

These stages were labeled as follows: Stage 1 as Cyclonic Storm (CS), Stage 2 as Severe Cyclonic Storm (SCS), & Stage 3 as Very Severe Cyclonic Storm (VSCS).

Further, to examine aerosol perturbations associated with Cyclone Vardah, the Modern-Era Retrospective Analysis for Research and Applications, Version 2 (MERRA-2) aerosol reanalysis product (M2T1NXAER) was utilized. This dataset provides hourly AOD at a spatial resolution of 0.5° × 0.625°. The AOD fields were extracted at 12:30 local time (07:00 UTC) for each day of the cyclone period (06–12 December 2016). The choice of local noontime was made to ensure consistency with satellite overpasses, as the MODIS sensors onboard Terra (~11:30 LT) and Aqua (~13:30 LT) satellites pass close to this time, thereby minimizing diurnal variability and ensuring temporal comparability between reanalysis and observations. For analysis, MERRA-2 aerosol species were classified into two categories: anthropogenic aerosols, consisting of black carbon (BC), organic carbon (OC), and sulphate (SO_4^{2-}), and natural aerosols, consisting of mineral dust (DU) and sea salt (SS). For each grid cell, the composite mean AOD for the period 06-13 December at 12:30 LT was calculated separately for total, anthropogenic, and natural components. Daily perturbations were then derived by subtracting this mean from each day's AOD, where positive anomalies indicated enhanced aerosol loading and negative anomalies represented reduced loading relative to the cyclone-period baseline.

3. Synoptic conditions of the VSCS 'Vardah'

The genesis of TC 'Vardah' can be traced back to a low-pressure area that developed over the south Andaman Sea and adjoining Sumatra on the morning of 4th December, 2016. It became a well-marked low-pressure area by the night of 5th December over the south Andaman Sea and adjoining southeast BoB. On 6th December, it intensified into a 'depression (D)' over the southeast BoB in the afternoon. Moving northwestwards initially and northwards thereafter, it intensified into a 'deep depression (DD)' by midnight of 7th December. The system further strengthened to a Cyclonic Storm (CS) named 'Vardah' on the morning of 8th December, and by midnight of 9th December, it intensified into a 'Severe Cyclonic Storm' (SCS). It then moved west-northwestwards and became a 'Very Severe Cyclonic Storm' (VSCS) over the southwest-central BoB on the evening of 10th December. Vardah reached its peak intensity of about 130 kmph on the evening of 11th December and maintained this intensity until noon of 12th December. Then, it weakened into an SCS at the time of landfall, crossing the north Tamil Nadu coast near Chennai between 1500-1700 hrs IST on 12th December 2016 with a wind speed of 110 kmph gusting to 125 kmph. Post-landfall, the SCS moved west-southwestwards, weakening into a CS in the evening, then into a DD by midnight, and into a depression by the early morning of 13th December. It continued to weaken into a well-marked low-pressure area by the forenoon of 13th December 2016. Fig. 1 shows the observed track of cyclone Vardah, according to IMD best track data, along with average PR during the period 6th to 12th December 2016. Further, it is to be noted that during its evolution, the cyclone progressed at an unusually slow pace. The 12-hour mean translational speed of the cyclone was only 5.2 km h^{-1}, well below the typical post-monsoon BoB average of 13 km h^{-1}. Such slower motion tends to extend the system's residence time over warm waters of

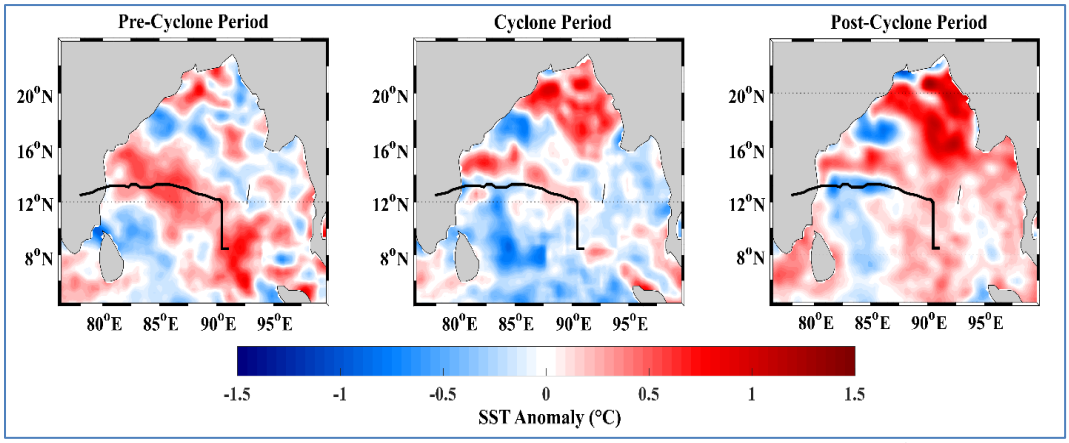

Fig. 2. SST anomalies (shaded, in °C) during pre-cyclone, cyclone, and post-cyclone period. The track of cyclone Vardah is represented by black solid curve

ocean, thereby favoring sustained air-sea fluxes that can contribute to intensification. In contrast, as the cyclone approached landfall, it underwent a marked acceleration, with translational speeds rising to about 15–20 km h^{-1}. The cyclone endured for nearly 159 hours (≈6.6 days), substantially longer than the post-monsoon climatological mean of 4.7 days for VSCS category over the NIO. Such an extended lifespan suggests enhanced ocean–atmosphere coupling, allowing greater accumulation of energy and moisture and consequently increasing the potential for prolonged hazardous impacts over both marine and terrestrial regions (The Accumulated Cyclone Energy (ACE), an indicator of the storm's overall intensity and damage potential, was estimated at 5.99×10^4 knot² for the TC Vardah).

4. Results

4.1. *Precipitation rate (PR) of TC vardah and the associated dynamical parameters*

A very high PR (~15 mm/hr) was observed along the storm track until the storm reached the SCS stage. Subsequently, as cyclone Vardah remained at its mature stage from December 8th to December 12th, the PR weakened and was observed to be lower (Fig. 1). From the figure, it can be inferred that as TC Vardah progressed, various processes may have contributed to the stabilization of its inner core, leading to a reduction in both the intensity and spatial extent of rainfall near the eyewall region. One significant factor could have been the eyewall replacement cycle, where TC Vardah could have developed a new outer eyewall that gradually contracted inward, replacing the original inner eyewall. This transition led to a temporary stabilization of the inner core, causing a decrease in rainfall intensity. Additionally, as TC Vardah moved across the BoB and approached the Indian coast, it encountered cooler SSTs and experienced upwelling of colder water due to its circulation (Fig. 2). Similar observations were reported by Ye *et al*. (2018). This reduction in SST limited the energy available for the storm, reducing convection and precipitation (6-7 mm/hr during landfall time) within the eyewall. Further, this specific behavior of TC Vardah could be influenced by various local and dynamic factors that could have contributed to the reduction in PR. Monitoring environmental conditions, such as wind shear, changes in atmospheric stability, and other atmospheric interactions, is necessary to observe the localized variations in rainfall patterns. The dynamical parameters that might have influenced the PR and the cyclone intensity have been analyzed further.

Dynamical parameters such as wind speed, relative vorticity (RV), CAPE, CIN, LTS, along with PR have been plotted to analyze their variation during the occurrence of TC Vardah (Fig. 3). Up until December 8th, 2016, right before cyclone Vardah became a SCS, the PR was observed to rise progressively. It is interesting to note that after reaching into the SCS stage, the PR was observed to decrease gradually (Fig. 3a). From 6th to 11th December, RV and wind speed were observed to rise steadily (Fig. 3b). Nevertheless, on December 11th, just before cyclone Vardah began to weaken, both the wind speed and RV started to reduce. A stable mechanism was observed during cyclone Vardah after the SCS stage, which prevented upward vertical motion of air, inhibiting the formation and development of deep convection. This can be inferred through rising LTS, and concurrent rise in CIN and fall in CAPE values after 9th December, Figs. 3(c & d). This prevalent stable condition after 9th December (i.e. after SCS stage) could have led to reductions in the PR. Further evidence of this stability, which reduced the PR, can be confirmed by examining the variations in wind speed, vertical winds, and relative humidity with height.

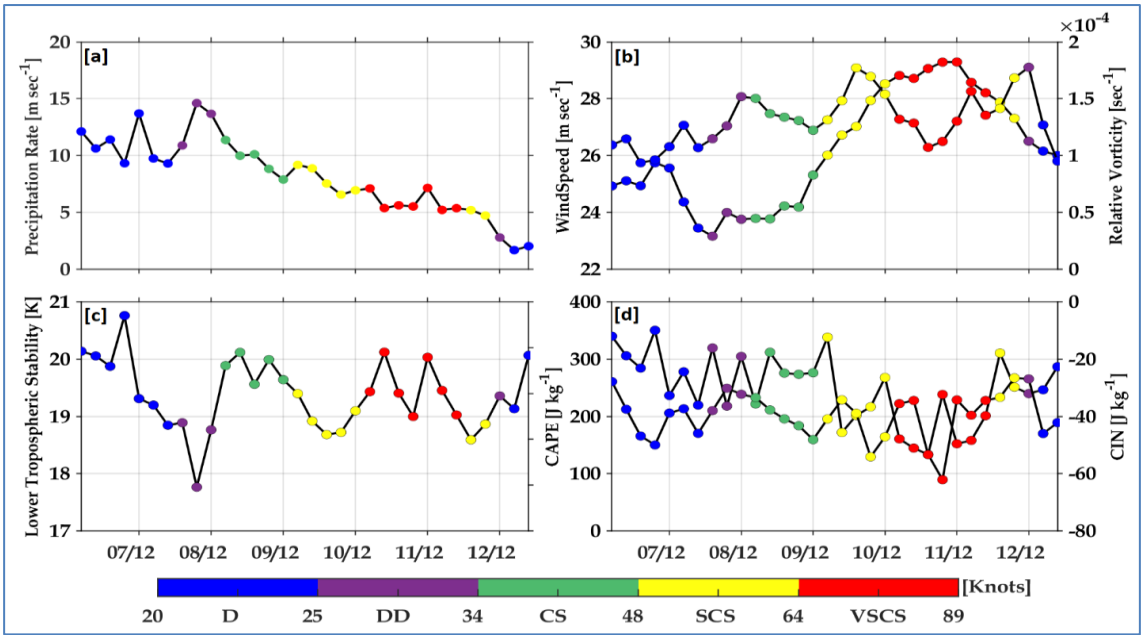

Figs. 3(a-d). Time series analysis of (a) Precipitation rate, (b) wind speed and relative vorticity (secondary Y-axis), (c) Lower Tropospheric Stability (LTS), and (d) CAPE and CIN (secondary Y-axis) during 6th – 12th December 2016. The colored stipples represent the stage of cyclone as represented by the color bar beneath the panels

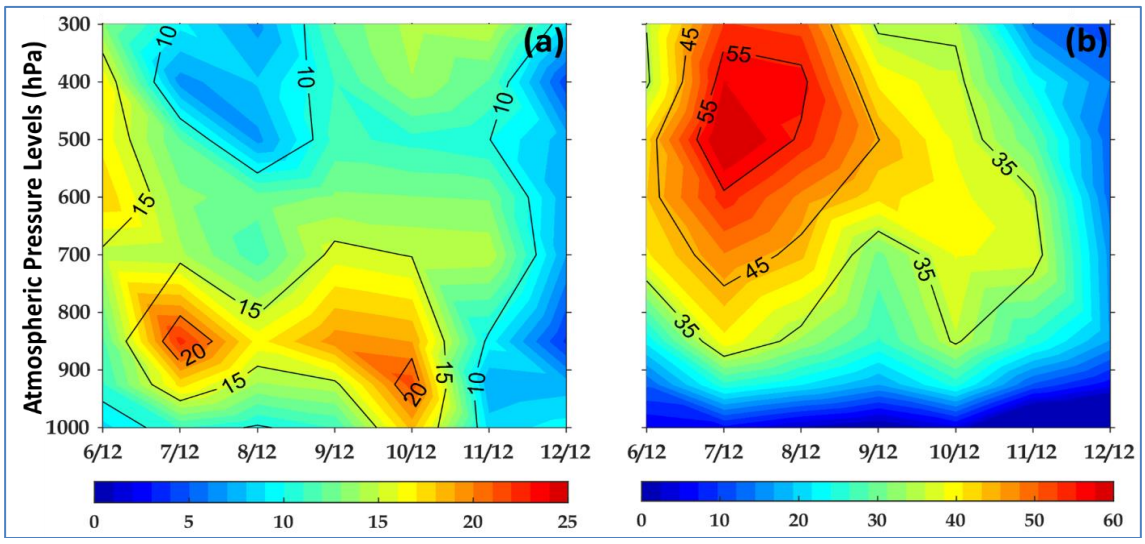

Figs. 4(a&b). Time-height cross-section of (a) wind speed (m/s), (b) vertical velocity (cm/s) in the eye of cyclone Vardah

4.2. *Time-height cross-section of wind speed and vertical winds*

It is evident that the maximum wind speed, reaching up to 25 m/s, extended to a height of nearly 2 km (~750 hPa) from the ground between December 7th and 10th, 2016 (Fig. 4a). However, after 10th December, wind speed started to reduce first near the surface, and this reduction became substantial over the whole column just before the landfall on 12th December. In the case of vertical winds, strong updrafts peaking up to 60 cm/s were observed till 8th December (up to SCS stage), which started reducing gradually afterward over the entire column till the landfall of Vardah. This reduction in vertical updraft is due to the stability governed by concurrent variation in CIN, CAPE, and LTS (Figs. 3c, d). Therefore, the wind speed and vertical wind observations are also indicative of reasons behind the reduction in the PR after the SCS stage of the cyclone Vardah, Figs. 4(a & b) and Fig. 3a.

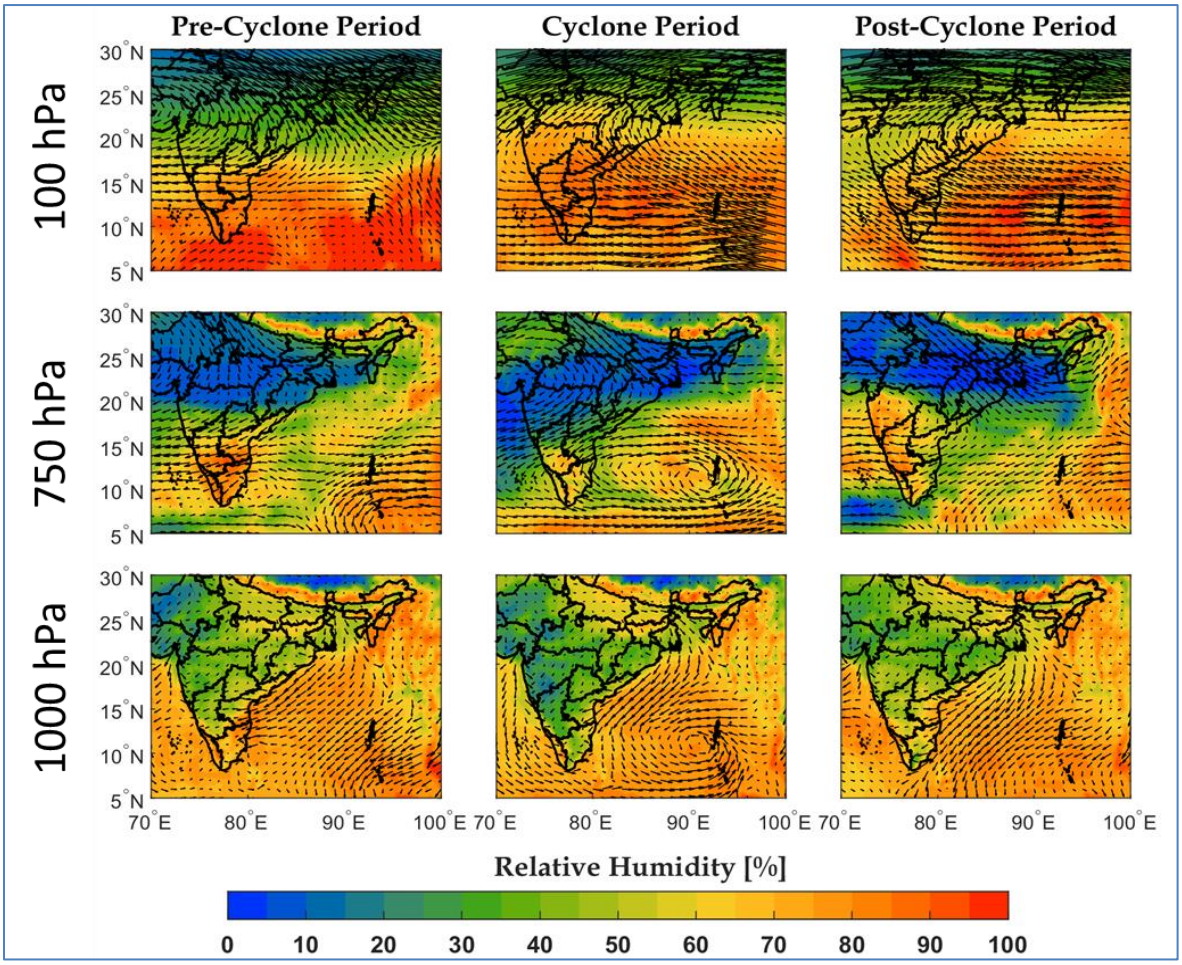

Fig. 5. Redistribution of moisture advection (i.e., relative humidity with wind vectors) at three different stages, including pre-, during, and post-cyclone, at three different pressure levels (1000, 750, 100 hPa from bottom to top) from GPM data products. The color bar indicates the magnitude of relative humidity (in percentage)

4.3. *Spatial variation of moisture advection*

Relative Humidity (RH) values in cyclones are typically associated with liquid water content below 8 km and with ice content above 8 km (Wu *et al.*, 2020). This distinction reflects the temperature and pressure conditions at different altitudes within the cyclone, where lower altitudes support liquid water clouds and higher altitudes, typically above the freezing level, contain ice-clouds. The RH, along with wind vectors, has been taken into consideration to observe their spatial variations during TC Vardah. Fig. 5 illustrates the changes in moisture loading (RH) at lower (1000 hPa), mid (750 hPa), and upper tropospheric levels (200 hPa) along with the wind vectors for the pre, during, and post-cyclone periods.

A strong presence of excessive moisture (RH ranging from 80% to 95%) in the lower troposphere was observed, with even higher values over the south and central BoB during both the pre-cyclonic and cyclonic periods (Fig. 5 third row). It is clearly evident that the TC Vardah was accompanied by notably high moisture advection, particularly from the southern part of the Indian coast at mid-tropospheric levels during the cyclone period (Fig. 5 second row). The intensification of cyclone Vardah led to increased moisture loading on the cyclone's periphery during the cyclonic period at mid-tropospheric levels (Fig. 5 second row). Additionally, at 100 hPa level a clear upper-level moisture divergence for the three cyclone periods (*i.e.*, pre, during and post cyclone periods) can be observed (Fig. 5 first row). Post-cyclone, the reduction in the RH was observed (Fig. 5 third column). The influx of moisture from the nearby region likely played a role in the initial intensification of Cyclone Vardah. However, the excess moisture and associated stability observed earlier may have also contributed to stabilizing the inner core, which could have reduced the potential for intensification after the SCS stage and before landfall. The high moisture loading and subsequent divergence likely influenced the cyclone's structure and precipitation patterns.

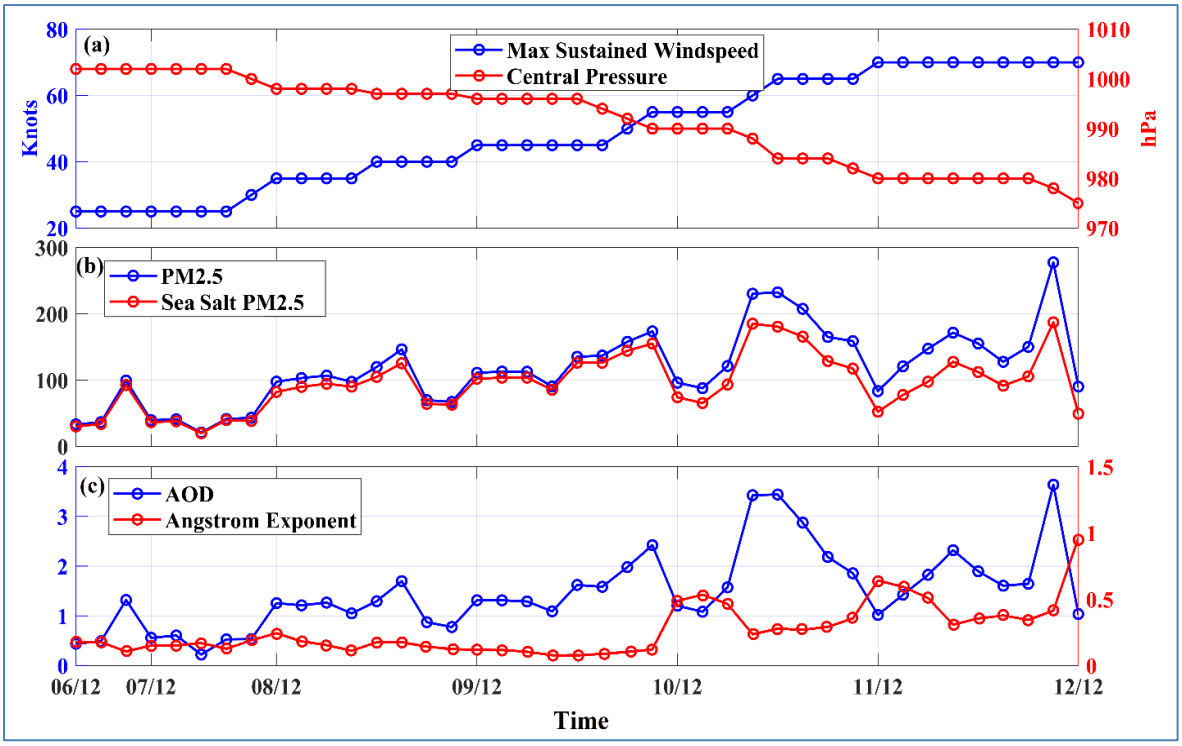

Figs. 6(a-c). (a) IMD provided observed maximum sustained wind (knots) and mean sea level pressure (Unit: hPa) during the life cycle of VSCS Vardah. (b) Surface PM2.5 concentration (blue curve; µg/m³) and sea salt concentration (red curve; µg/m³) during the same period. (c) Area-averaged Aerosol Optical Depth (AOD, blue curve) and Angstrom Exponent (AE, red curve) over the same period

Furthermore, the interaction of TC Vardah with aerosols could have significant implications. Aerosols can affect cloud microphysics by acting as Cloud Condensation Nuclei (CCN) or Ice Nuclei (IN), potentially altering cloud formation, precipitation efficiency, and intensity (Andreae, *et al*. 2008; Tao *et al.,* 2012). Increased aerosol concentrations can lead to smaller cloud droplets, delaying coalescence and precipitation, which could further explain the observed reduction in PR as observed during the cyclone evolution.

4.4. *Time series analysis of aerosol variables along the track*

During the evolution of VSCS Vardah from 6th to 12th December 2016, a marked intensification of the cyclone was observed, characterized by a significant decrease in mean sea level pressure (MSLP) and an increase in maximum sustained winds (Fig. 6a). Alongside this intensification, a progressive increase in various aerosol parameters was recorded along the cyclone's track up to the point of landfall (12th December 2016). Specifically, there was a notable rise in AOD, sea salt $PM_{2.5}$, surface PM2.5, and the AE after 8th or 9th December when cyclone reached SCS stage, Figs. 6(b & c). The elevated AOD indicates a higher concentration of aerosols in the atmosphere, while the increase in sea salt $PM_{2.5}$ and surface $PM_{2.5}$ points to a substantial presence of particulate matter originating from both marine and terrestrial sources. The rising AE suggests a dominance of smaller aerosol particles, which can have significant implications on cloud microphysics and radiative properties associated with TC Vardah. This progressive accumulation of aerosols along the cyclone's path likely contributed to the modification of the cloud structure and dynamics, potentially reducing the precipitation efficiency of the TC as observed after SCS stage (refer to Fig. 3a). Furthermore, the source of aerosols and their distribution before, during, and after the cyclone Vardah have been explored in the next section.

4.5. *Spatial distribution of AOD and rainfall during different phases of cyclone Vardah*

During the pre-cyclonic period, higher concentrations of aerosols can be observed over the Indian subcontinent, especially over the Indo-Gangetic region. This might be attributed to the cold surface temperatures combined with calm winds, a shallow boundary layer, and high aerosol emission rates, as well as dense fog, mist, or haze, commonly observed in northern India during winter, particularly over the Central and Eastern Indo-Gangetic Plain (Kumar *et al.*, 2015; Balaji *et al.*, 2018; Manoj *et al.*,

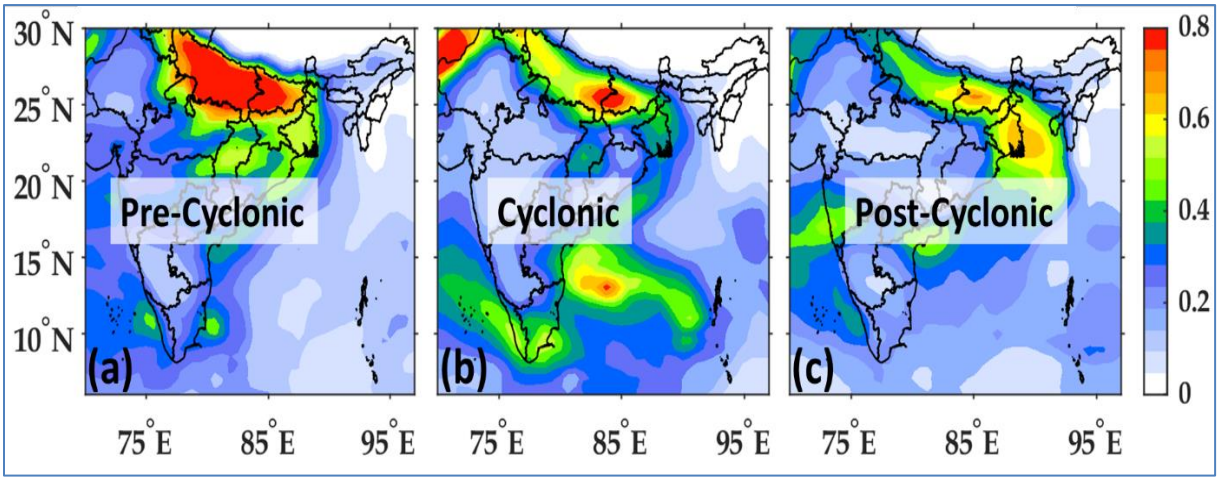

Figs. 7(a-c). Spatial variation of averaged AOD obtained from MODIS data products for different cyclonic periods

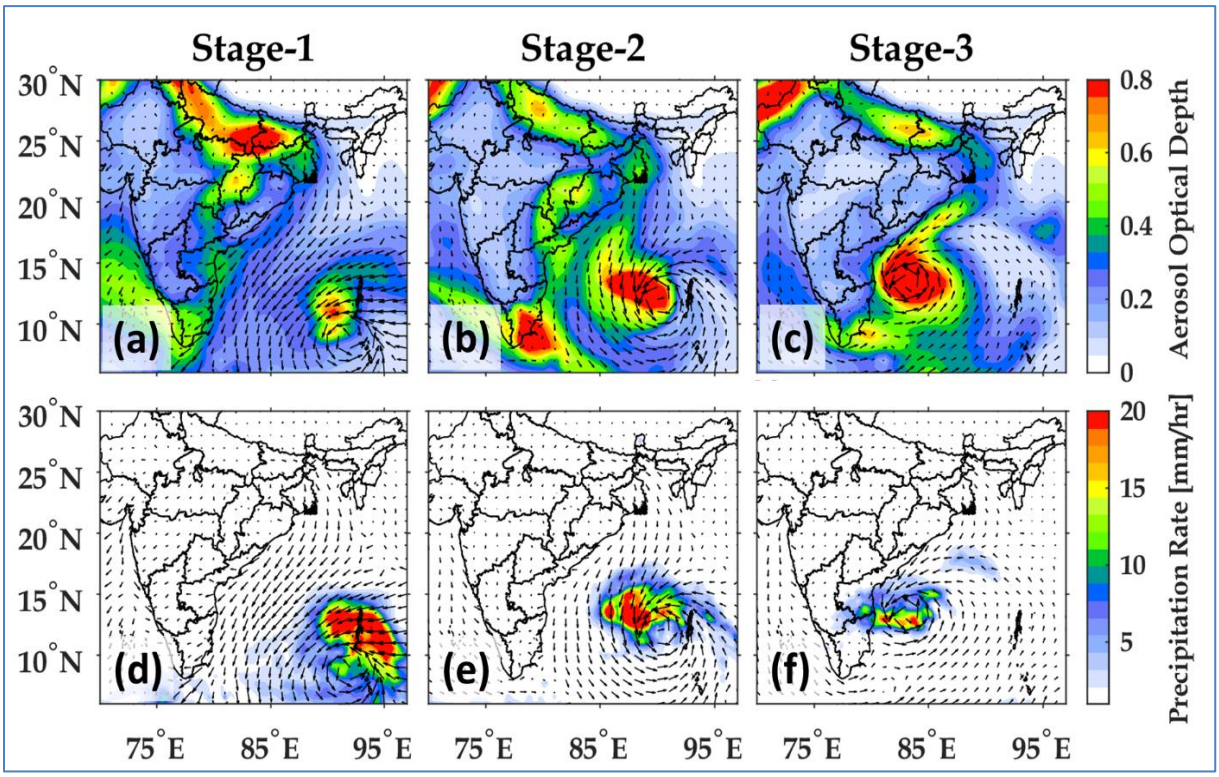

Figs. 8(a-f). Spatial variation of averaged AOD (i.e. figure 8 (a-c)) and precipitation rate (mm/hr; figure 8 (d-f))) from GPM data product for stage-1 (CS), stage-2 (SCS), and stage-3 (VSCS) respectively overlaid with 850 hPa wind vectors

2019). Also, with a dominant northwesterly flow over north India, aerosol loading was observed to be significantly higher (AOD ~ 0.8) over the Indo-Gangetic plain region in the pre-cyclonic period (Fig. 7).

During the cyclonic period, the influx of aerosols can be seen into the cyclone region from the Indo-Gangetic region. This influx is achieved by the enhanced northwesterly winds before and during the cyclone. Also, these cyclonically rotating winds seemed to drag the aerosols from the nearby region towards the cyclone center (Fig. 7). Also, due to the intensification of the cyclone, the sea salt $PM_{2.5}$ increment was observed because of the associated strong winds

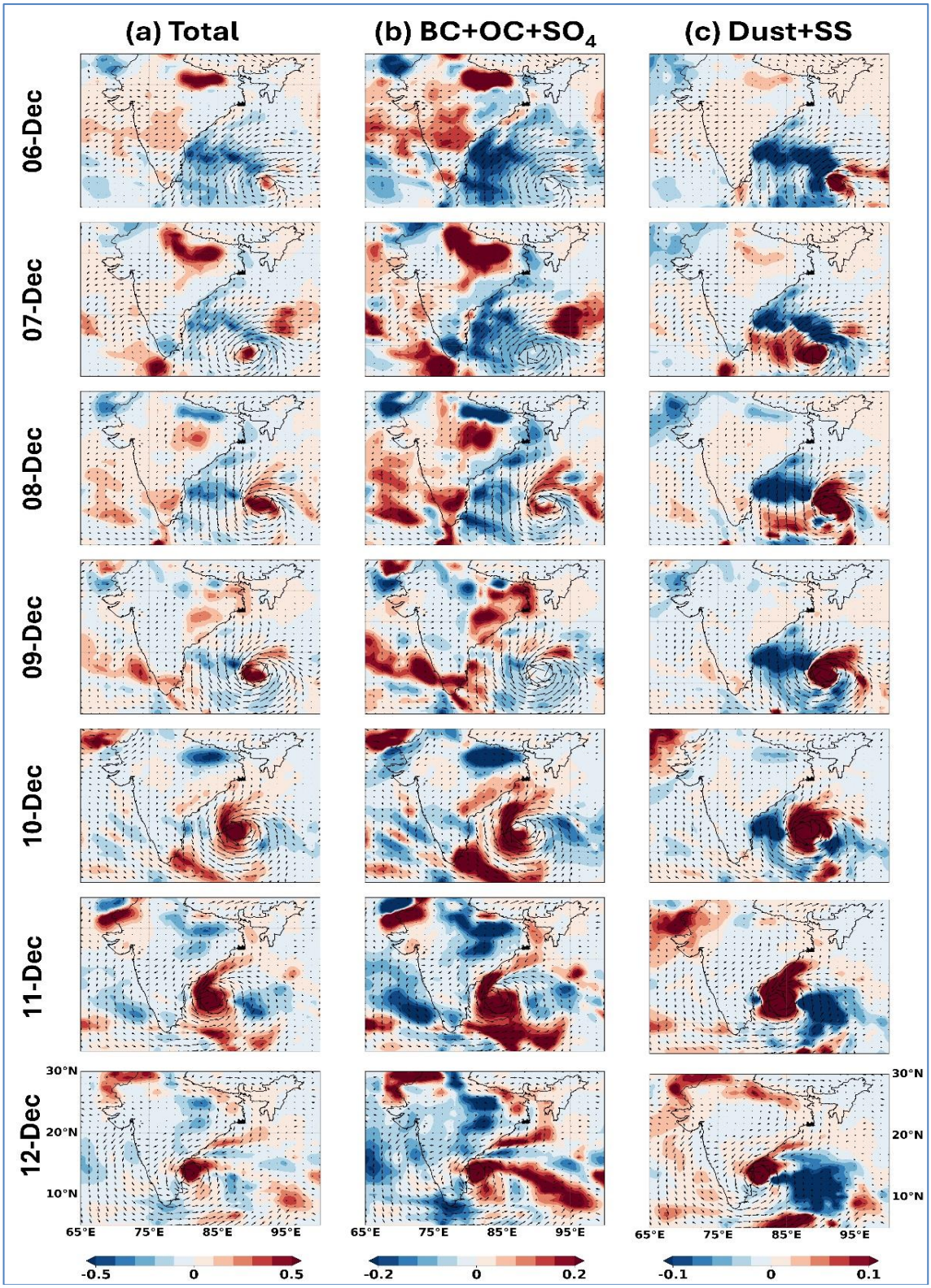

Figs. 9(a-c). Changes in aerosol loading from MERRA-2 at 12:30 h local time during 6–12 December 2016 associated with Cyclone Vardah: (a) Total AOD, (b) anthropogenic AOD (Black Carbon + Organic Carbon + Sulphate, with sulphate scaled by 1.375), and (c) natural AOD (Dust + Sea Salt). The anomalies highlight cyclone-induced perturbations in aerosol distributions over the Bay of Bengal and adjoining regions

(refer to Fig. 6b). In addition to aerosols being dragged from the Indo-Gangetic Plain towards the center of the cyclone, aerosols off the east coast of southern India were also advected eastward.

It is noteworthy that during the post-cyclonic period, aerosol loading decreased over the Indo-Gangetic Plain while increasing over central-eastern India and off the east coast compared to the pre-cyclonic period. This indicates that cyclone Vardah, through its circulation and wind patterns, transported the contaminated air-mass from the Indo-Gangetic Plain towards the east coast.

As the aerosols appear to be driven by the cyclonic circulation and the nearby winds throughout the cyclone period, we further investigated the distribution of aerosols during the three different stages of the cyclonic period (i.e. CS, SCS, VSCS). Along with AOD, we have also observed the rainfall patterns during these stages that might have been modulated by the strong variability of observed aerosol loading. Stage 1 (CS), when the cyclone was near Andaman, exhibits a comparatively high aerosol loading over the Indo-Gangetic plain region because of stable atmospheric conditions, such as temperature inversions and limited vertical mixing, which trapped and accumulated the pollutants and aerosols closer to the surface (Kumar *et al.,* 2015; Balaji *et al.,* 2018; Manoj *et al.,* 2019). Also, a high AOD near the cyclone was evident during stage 1, which could be due to sea salt loaded into the atmosphere by strong cyclonic winds. Also, during stage 1, the PR was observed to be higher than in any other stage (Fig. 8, first column).

The movement of aerosol from the Indo-Gangetic Plain towards the BoB during Stage-2 (SCS) was assisted by dynamic and turbulent environmental conditions associated with cyclone Vardah along with the dominant northwesterly. During this influx of aerosol, reduction in area of high PR was observed (Fig. 8 second column). As the cyclone Vardah further intensified to VSCS and approached the coast, increased sea spray aerosols were observed due to interaction with the ocean surface (Fig. 8 third column and Fig. 6c). The strong winds associated with the cyclone caused large waves and enhanced turbulence, resulting in the production of sea salt aerosols. These aerosols contribute to the overall aerosol loading near the coastal areas during the VSCS stage of the cyclone, which could be responsible for the enhancement of aerosol loading over the Chennai region discussed in the next section, Figs. (9 & 10).

Aerosol concentrations gradually increase from Stage 1 to Stage 3 over BoB, which inhibits the development and intensification of convective clouds by hindering the vertical transport of heat and moisture. Aerosol particles disrupt the atmosphere's stability and buoyancy, which makes convection more difficult to maintain. This causes PR to decrease over time, as evidenced by the gradual decay of the precipitation core from Stage 1 to Stage 3 until it reaches the coast (refer to Fig. 3a).

4.6. *Anomalies in anthropogenic and natural aerosols during cyclone Vardah*

Fig. 9 depicts the spatio-temporal anomalies in aerosol loading along with winds during 6-12 December 2016, capturing the evolution of the cyclone Vardah. During the early phase (6-8 December), when the storm was developing over the BoB, strong positive anomalies in total AOD (0.2 to 0.5) were observed along the cyclone's path, indicating vertical redistribution of aerosols by advection and vigorous convection. At the same time, enhanced anthropogenic aerosol loading was retained over the Indo-Gangetic plain region and central India, with positive anomalies (~ +0.2) suggesting that the cyclone's outer circulation transported polluted continental air masses eastward towards the Bay. Natural aerosols exhibited a relatively weak signal during this stage, although some enhancement in sea salt was evident over the southern Bay, consistent with the strengthening low-level winds.

As the cyclone intensified and approached landfall (9-12 December), the contrast between aerosol types became more pronounced. Anthropogenic aerosol species (BC, OC, and SO_4^{2-}) showed strong depletion in the cyclone's eyewall and adjoining marine regions up to 6–10 December, primarily due to wet scavenging and convective dilution, while their concentrations were higher along the periphery of the system and over the Indo-Gangetic Basin, reflecting large-scale advection. In contrast, natural aerosols displayed a marked enhancement, with sea salt loading reaching positive anomalies of nearly +0.1 along the storm track, driven by intense surface winds and wave activity. Dust contributions remained negligible, with weak negative signals over western India, indicating that entrainment from desert regions was not significant during this event. The spatial dipole-suppressed anthropogenic loading near the storm center and enhanced natural aerosols over the Bay, coupled with outward transport of continental pollution, clearly demonstrates the cyclone's role as both a cleansing agent and a redistributor of aerosols. After landfall, the residual circulation continued to advect pollutants toward northern and central India, highlighting how TCs can perturb aerosol distributions over large spatial scales and affect regions far from the landfall zone.

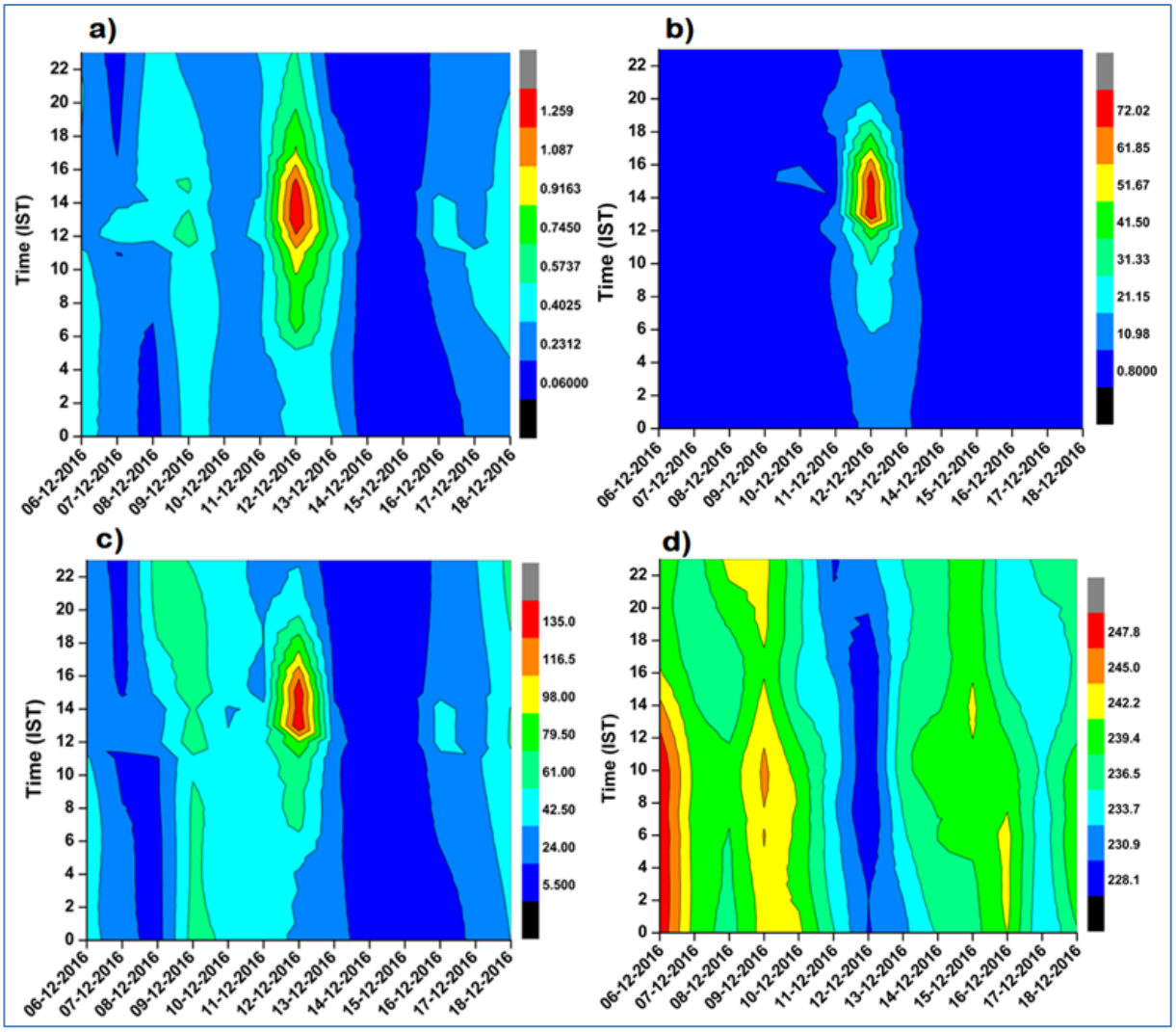

Figs. 10(a-d). Area averaged (1° x 1°) 'date (x axis)-time (y-axis)' values of aerosol variables (a) AOD (unitless) (b) sea salt concentration (µg m^{-3}) (c) $PM_{2.5}$ concentration (µg m^{-3}) (d) Total ozone content (Dobson unit) over Chennai (Landfall point)

4.7. *Area-averaged aerosol variables over landfall point (Chennai)*

During the landfall of Cyclone Vardah on December 12th, 2016, over Chennai, significant atmospheric changes were observed in terms of aerosol and ozone dynamics, as illustrated in Fig. 10. The AOD peaked at nearly 1.3 between 11 to 16 IST, indicating a substantial increase in aerosol loading due to the cyclone's strong winds and sea spray (Fig. 10a). During this period, the sea salt concentrations rose to approximately 72 µg m^{-3}, reflecting the marine influence brought inland by the cyclone (Fig. 10b). Concurrently, surface $PM_{2.5}$ concentrations surged to about 135 µg m^{-3}, suggesting the combined effect of marine aerosols and re-suspended particulates due to the turbulent cyclone conditions (Fig. 10c). Additionally, the total ozone content dropped to 228 Dobson units during 2 to 16 IST on the day of landfall (Fig. 10d). This decrease is likely caused by the convective mixing and redistribution of ozone within the atmospheric column associated with the cyclone's dynamical processes. These observations highlight cyclone Vardah's profound impact on aerosol distribution and atmospheric composition, underscoring the intricate interactions between TCs and regional air quality.

5. Conclusions

The study primarily aimed to evaluate the impact of aerosols and other dynamic factors on the precipitation induced by cyclone Vardah. This focus stemmed from

the cyclone's unusual behaviour, as it produced only 5 mm/hr of rainfall, even being a VSCS at landfall on the eastern coast of India.

The intensity of the precipitation increased eventually as cyclone Vardah moved from depression to SCS. The PR, however, started gradually declining prior to Vardah reaching at VSCS, *i.e*, maturity stage. This observed unusual reduction of precipitation is linked to the enhanced LTS, reduced CAPE, and elevated CIN during and after the SCS stage, leading to enhanced stability of the atmospheric column. Moreover, during the SCS, the polluted air mass at the Indo-Gangetic plain was dragged towards the BoB into the cyclone by the northwesterly wind that was blowing over the Indian subcontinent. Aerosol loading was observed to be higher in stage 2 (SCS) and stage 3 (VSCS) of cyclonic period, which was responsible for restricting intensification of convective clouds. The spatial variability of TC precipitation was quite opposite to the spatial variability of aerosol loading in different Stage 1 (SC) to Stage 3 (VSCS). The reanalysis data indicated that the influx of dry air into the middle troposphere coincided with the decline in the PR near the coast during TC Vardah's landfall. Aerosol particles disrupt the atmosphere's stability and buoyancy, which makes convection more difficult to maintain. Also, during and after the landfall, the redistribution of aerosol from the Indo-Gangetic region to the east coast of India was observed, leading to increased aerosol concentration over Chennai.

The background conditions suggest the presence of aerosol loading during the intensification of cyclone Vardah from SCS to VSCS intensity stage, which in turn modulated the precipitation observed during the cyclone. This phenomenon, known as the 'aerosol indirect effect', can modulate atmospheric stability, circulation, and convective processes associated with the TCs.

Additionally, spatio-temporal aerosol anomalies during 6-12 December highlight the cyclone's dual role as a cleansing agent and redistributor of aerosols. Anthropogenic aerosols were depleted near the storm core due to wet scavenging, while sea salt aerosols were enhanced along the storm track and polluted continental air masses were transported eastward by the outer circulation. This contrast between suppressed anthropogenic and enhanced natural aerosols highlights the complex feedbacks between cyclones and aerosol distributions over land and ocean.

During the landfall of the TC Vardah on 12 December 2016 over Chennai, the AOD peaked at about 1.3, sea-salt concentrations rose to nearly 72 $\mu g\ m^{-3}$, and surface $PM_{2.5}$ reached around 135 $\mu g\ m^{-3}$, reflecting increased marine aerosol transport and re-suspension under turbulent conditions. Simultaneously, the total ozone content decreased to 228 Dobson Units during 02–16 IST, likely due to convective mixing and redistribution. These observations highlight the cyclone's pronounced influence on aerosol loading and atmospheric composition, underscoring the complex interactions between tropical cyclones, air quality, and regional climate. Though this study strives to link the changes in aerosol with the rainfall variability induced by cyclones, a modeling study in this regard in future could prove beneficial.

Acknowledgement

We acknowledge IMD (India Meteorological Department) for providing the best-track data and rainfall data associated with the VSCS Vardah, which were crucial for this research. All the authors sincerely thank their respective Heads, Principals, and Directors of their institutions for their support and guidance, which facilitated the collaborative efforts between the first author and co-authors in making this work possible. We extend our sincere acknowledgement to NASA, the National Aeronautics and Space Administration, for freely providing essential data to conduct our study.

Data Availability

The main data used in this paper are the ERA5 reanalysis data and from ECMWF. The hourly pressure-level and surface-level meteorological data of ERA5 were used (source: https://cds.climate. copernicus.eu/cdsapp#!/dataset/reanalysis-era5-single-levels?tab=form,).
Parameters are listed in Table 1. The NASA Earth Observing System Data and Information System (EOSDIS) has three product levels that are used to organize and archive GPM data products at the GES DISC. This system uses a grid-point statistical interpolation analysis system (Liu *et al.,* 2017).

Declaration of interests

The authors declare that they have no known competing financial interests or personal relationships that could have appeared to influence the work reported in this manuscript.

Author statement

The contents and views expressed in this research paper/article are the views of the authors and do not necessarily reflect the views of the organizations they belong to". This work is entirely original and has not been

Author's Contributions

Vivek Singh: Conceptualization; Formal analysis; Visualization; Roles/Writing - original draft; and Writing - review & editing.
Hitesh Gupta: Formal Analysis, Visualization, Software, Writing – review & editing;
Arun Kumar: Visualization, Software,
Amarendra Singh: Visualization, Software;
Sumit Singh: Visualization, Software
Bhagyalaxmi Verma: Data curation; Formal analysis; Visualization, Software
Charu Jhamaria: Supervision; Validation;
Gaurav Tiwari: Formal analysis; Visualization,
Ashish Routray**:** Validation,
Dileep Kumar Gupta**:** Validation,
Abhishek Lodh**:** Validation.
Arpan Bhattacharjee: Visualization, Software

Disclaimer: The contents and views presented in this research article/paper are the views of the authors and do not necessarily reflect the views of the organizations they belong to.

References

Andreae, M.O. and Rosenfeld, D.J.E.S.R., 2008, "Aerosol–cloud–precipitation interactions", Part 1. The nature and sources of cloud-active aerosols. *Earth-Science Reviews*, **89**, 1-2, 13-41.

Balaguru, K., Foltz, G.R., Leung, L.R. and Hagos, S.M., 2022, "Impact of rainfall on tropical cyclone-induced sea surface cooling", *Geophysical Research Letters*, **49**, 10, p.e2022GL 098187.

Balaji, M., Chakraborty, A. and Mandal, M., 2018, "Changes in tropical cyclone activity in north Indian Ocean during satellite era (1981–2014)", *International Journal of Climatology*, **38**, 6, 2819-2837.

Betsy, K.B., Mehta, S.K., Ananthavel, A., Kakkanattu, S.P., Purushotham, P., Seetha, C.J. and Peediakal, M.P., 2024, "Roles of tropical cyclones with varying intensities in the re-distribution of aerosols", *Atmospheric Pollution Research*, **15**, 2, p.101990.

Bhavithra, R. S. and Sannasiraj, S. A. 2022, "Climate change projection of wave climate due to Vardah cyclone in the Bay of Bengal." *Dyn.* Atmos. Oceans, **97**, 101279.

Busireddy, N.K.R., Ankur, K., Osuri, K.K., Sivareddy, S. and Niyogi, D., 2019, "The response of ocean parameters to tropical cyclones in the Bay of Bengal:, *Quarterly Journal of the Royal Meteorological Society*, **145**, 724, 3320-3332.

Cheriyan, E., Rao, A.R. and Sanilkumar, K.V., 2022, "Response of sea surface temperature, chlorophyll and particulate organic carbon to a tropical cyclonic storm over the arabian sea, southwest india", *Dynamics of Atmospheres and Oceans*, **97**, p.101287.

Chiacchio, M., Pausata, F.S., Messori, G., Hannachi, A., Chin, M., Önskog, T., Ekman, A.M. and Barrie, L., 2017, "On the links between meteorological variables, aerosols, and tropical cyclone frequency in individual ocean basins", *Journal of Geophysical Research: Atmospheres*, 122, 2, 802-822.

Cotton, W.R., Krall, G.M. and Carrió, G.G., 2012, "Potential indirect effects of aerosol on tropical cyclone intensity: Convective fluxes and cold-pool activity. *Tropical Cyclone research and review*, **1**, 3, pp.293-306.

Dee, D.P., Uppala, S.M., Simmons, A.J., Berrisford, P., Poli, P., Kobayashi, S., Andrae, U., Balmaseda, M.A., Balsamo, G., Bauer, D.P. and Bechtold, P., 2011. The ERA-Interim reanalysis: Configuration and performance of the data assimilation system. *Quarterly Journal of the royal meteorological society*, **137**, 656, .553-597.

Diao, C., Xu, Y. and Xie, S.P., 2021, "Anthropogenic aerosol effects on tropospheric circulation and sea surface temperature (1980–2020): separating the role of zonally asymmetric forcings", *Atmospheric Chemistry and Physics*, **21**, 24, pp.18499-18518.

Evan, A.T., Kossin, J.P., 'Eddy'Chung, C. and Ramanathan, V., 2011, "Arabian Sea tropical cyclones intensified by emissions of black carbon and other aerosols", *Nature*, **479**, 7371, pp.94-97.

Garner, A.J., 2023, "Observed increases in North Atlantic tropical cyclone peak intensification rates. *Scientific Reports*, **13**, 1, p.16299.

Gupta, H., Deogharia, R., Sil, S., Singh, V. and Ray, A., 2025, "On the interconnection of marine heatwaves and the extremely severe cyclonic storms Mocha and Biparjoy in the Northern Indian Ocean", *Natural Hazards*, pp.1-21.

Gupta, H., Sil, S., Gangopadhyay, A. and Gawarkiewicz, G., 2024, "Observed surface and subsurface Marine Heat Waves in the Bay of Bengal from in-situ and high-resolution satellite data", *Climate Dynamics*, **62**, 1, pp.203-221.

Gramer, L.J., Zhang, J.A., Alaka, G., Hazelton, A. and Gopalakrishnan, S., 2022, "Coastal downwelling intensifies landfalling hurricanes", *Geophysical research letters*, **49**, 13, p.e2021GL096630.

Hendricks, E.A., Braun, S.A., Vigh, J. L. and Courtney, J.B., 2019, "A summary of research advances on tropical cyclone intensity change from 2014-2018", *Tropical Cyclone Research and Review*, **8**, 4, pp.219-225.

Herbener, S.R., Van Den Heever, S.C., Carrió, G.G., Saleeby, S.M. and Cotton, W.R., 2014, "Aerosol indirect effects on idealized tropical cyclone dynamics", *Journal of the Atmospheric Sciences*, **71**, 6, pp.2040-2055.

Kompalli, S.K., Babu, S.N.S., Moorthy, K.K., Satheesh, S.K., Gogoi, M.M., Nair, V.S., Jayachandran, V.N., Liu, D., Flynn, M.J. and Coe, H., 2021, "Mixing state of refractory black carbon aerosol in the South Asian outflow over the northern Indian Ocean during winter", *Atmospheric Chemistry and Physics*, **21**, 11, 9173-9199.

Kumar, H. and Tiwari, S., 2023, "Aerosol loading over the Northern Indian Ocean using space-borne measurements", In *Atmospheric Remote Sensing* (pp. 191-210). Elsevier.

Kumar, R., Barth, M.C., Nair, V.S., Pfister, G.G., Suresh Babu, S., Satheesh, S.K., Krishna Moorthy, K., Carmichael, G.R., Lu, Z. and Streets, D.G., 2015, "Sources of black carbon aerosols in South Asia and surrounding regions during the Integrated Campaign for Aerosols, Gases and Radiation Budget (ICARB)", *Atmospheric Chemistry and Physics*, **15**,10,5415-5428.

Kumari, V.R., Sarma, V.V.S.S., Mahesh, G. and Sudheer, A.K., 2022, "Temporal variations in the chemical composition of aerosols over the coastal Bay of Bengal", *Atmospheric Pollution Research*, **13**, 2, p.101300.

Kumari, V.R., Sarma, V.V.S.S. and Kumar, M.D., 2022, "Spatial variability in aerosol composition and its seawater acidification potential in coastal waters of the western coastal Bay of Bengal", *Journal of Earth System Science*, **131**, 4, p.251.

Lin, Y., Wang, Y., Hsieh, J.S., Jiang, J., Su, Q. and Zhang, R., 2023, "Assessing the destructiveness of tropical cyclone by anthropogenic aerosols under an atmosphere-ocean coupled framework", *EGUsphere*, *2023*, pp.1-48.

Liu, Z., Ostrenga, D., Vollmer, B., Deshong, B., Macritchie, K., Greene, M. and Kempler, S., 2017, "Global precipitation measurement mission products and services at the NASA GES DISC", *Bulletin of the American Meteorological Society*, **98**, 3, 437-444.

Luo, H., Jiang, B., Li, F. and Lin, W., 2019, "Simulation of the effects of sea-salt aerosols on the structure and precipitation of a developed tropical cyclone", *Atmospheric research*, **217**, 120-127.

Mandal, S., Sil, S., Shee, A. and Venkatesan, R., 2018, "Upper ocean and subsurface variability in the Bay of Bengal during cyclone Roanu: A synergistic view using in situ and satellite observations", *Pure and Applied Geophysics*, **175**, 4605-4624.

Manoj, M.R., Satheesh, S.K., Moorthy, K.K., Gogoi, M.M. and Babu, S.S., 2019, "Decreasing trend in black carbon aerosols over the Indian region", *Geophysical Research Letters*, **46**, 5, 2903-2910.

Murakami, H., 2022, "Substantial global influence of anthropogenic aerosols on tropical cyclones over the past 40 years", *Science advances*, **8**, 19, p.eabn9493.

Nair, A., Das, S.S., Thomas, A., Sarangi, C. and Kanawade, V.P., 2020, "Role of Cyclone "Ockhi" in the re-distribution of aerosols and its impact on the precipitation over the Arabian Sea", *Atmospheric research*, **235**, p.104797.

Panda, J., Sarkar, A. and Giri, R.K., Atmospheric aerosols and their effects on radiation, clouds, and precipitation in different meteorological scenarios.

Pravia-Sarabia, E., Gómez-Navarro, J.J., Jiménez-Guerrero, P. and Montávez, J.P., 2021, "Influence of sea salt aerosols on the development of Mediterranean tropical-like cyclones", *Atmospheric Chemistry and Physics*, **21**, 17, pp.13353-13368.

Rajasree, V.P.M., Kesarkar, A.P., Bhate, J.N., Singh, V., Umakanth, U. and Varma, T.H., 2016, "A comparative study on the genesis of North Indian Ocean tropical cyclone Madi (2013) and Atlantic Ocean tropical cyclone Florence (2006)", *Journal of Geophysical Research: Atmospheres*, **121**, 23, 13-826.

Rathore, S., Goyal, R., Jangir, B., Ummenhofer, C.C., Feng, M. and Mishra, M., 2022, "Interactions between a marine heatwave and Tropical Cyclone Amphan in the Bay of Bengal in 2020", Frontiers in Climate, **4**, p.861477.

Reale, O., Lau, K.M., Da Silva, A. and Matsui, T., 2014, "Impact of assimilated and interactive aerosol on tropical cyclogenesis", *Geophysical Research Letters*, **41**, 9, 3282-3288.

Sarkar, A., Amal, K.K., Sarkar, T., Panda, J. and Paul, D., 2021, "Variability in air-pollutants, aerosols, and associated meteorology over peninsular India and neighboring ocean regions during COVID-19 lockdown to unlock phases", *Atmospheric Pollution Research*, **12**, 12, p.101231.

Sengupta, D., Goddalehundi, B. R. and Anitha, D. S., 2008, "Cyclone-induced mixing does not cool SST in the post-monsoon north Bay of Bengal", *Atmospheric Science Letters*, **9**, 1, 1-6.

Sil, S., Gangopadhyay, A., Gawarkiewicz, G. and Pramanik, S., 2021, "Shifting seasonality of cyclones and western boundary current interactions in Bay of Bengal as observed during Amphan and Fani" *Scientific Reports*, **11**, 1, p.22052.

Singh, K.S., Thankachan, A., Thatiparthi, K., Reshma, M.S., Albert, J., Bonthu, S. and Bhaskaran, P.K., 2022, "Prediction of rapid intensification for land-falling extremely severe cyclonic storms in the Bay of Bengal", *Theoretical and Applied Climatology*, 1-19.

Singh, V., Srivastava, A.K., Samanta, R., Singh, A., Kumar, A. and Singh, A.K., 2023, "Investigating Physics Behind the Rapid Intensification and Catastrophic Landfall of Cyclone 'Titli'(2018) in the Bay of Bengal", *Indian Journal of Pure & Applied Physics (IJPAP)*, **61**, 3, 175-181.

Singh, V.K. and Roxy, M.K., 2022, "A review of ocean-atmosphere interactions during tropical cyclones in the north Indian Ocean", *Earth-Science Reviews*, **226**, p.103967.

Tao, W.K., Chen, J.P., Li, Z., Wang, C. and Zhang, C., 2012, "Impact of aerosols on convective clouds and precipitation", *Reviews of Geophysics*, **50**, 2.

Tiwari, G., Kumar, P., Javed, A., Mishra, A.K. and Routray, A., 2022, "Assessing tropical cyclones characteristics over the Arabian Sea and Bay of Bengal in the recent decades", *Meteorology and Atmospheric Physics*, **134**, 3, p.44.

Tiwari, G., Kumar, P. and Tiwari, P., 2022, "The appraisal of tropical cyclones in the North Indian Ocean: An overview of different approaches and the involvement of Earth's components", *Frontiers in Earth Science*, **10**, p.823090.

Ventura, A., Simões, E.F., Almeida, A.S., Martins, R., Duarte, A.C., Loureiro, S. and Duarte, R.M., 2021, "Deposition of aerosols onto upper ocean and their impacts on marine biota", *Atmosphere*, **12**, 6, p.684.

Wadler, J.B., Rudzin, J.E., de la Cruz, B.J., Chen, J., Fischer, M., Chen, G., Qin, N., Tang, B. and Li, Q., 2023, "A review of recent research progress on the effect of external influences on tropical cyclone intensity change", *Tropical Cyclone Research and Review*.

Wang, Y., Lee, K.H., Lin, Y., Levy, M. and Zhang, R., 2014, "Distinct effects of anthropogenic aerosols on tropical cyclones", *Nature Climate Change*, **4**, 5, 368-373.

Wu, S.N., Soden, B.J. and Alaka Jr, G.J., 2020, "Ice water content as a precursor to tropical cyclone rapid intensification. *Geophysical Research Letters*, **47**, 21, p.e2020GL089669.

Yadav, K., Rao, V.D., Sridevi, B. and Sarma, V.V.S.S., 2021, "Decadal variations in natural and anthropogenic aerosol optical depth over the Bay of Bengal: the influence of pollutants from Indo-Gangetic Plain", *Environmental Science and Pollution Research*, **28**, 39, 55202-55219.

Yamada, H., Moteki, Q. and Yoshizaki, M., 2010, "The unusual track and rapid intensification of Cyclone Nargis in 2008 under a characteristic environmental flow over the Bay of

Bengal", *Journal of the Meteorological Society of Japan. Ser. II*, **88**, 3, 437-453.

Yang, X., Zhou, L., Zhao, C. and Yang, J., 2018, "Impact of aerosols on tropical cyclone-induced precipitation over the mainland of China. *Climatic Change*, **148**, 173-185.

Ye, H., Kalhoro, M.A., Sun, J. and Tang, D., 2018, "Chlorophyll blooms induced by tropical cyclone Vardah in the Bay of Bengal", *Indian J. Geo-Mar. Sci*, **47**, 1383-1390.

Zhang, Y., Zhao, X. and Zhang, H.M., 2023, "Relationship between the aerosol loadings over the Bay of Bengal and the Arabian Sea in the early summer and Asian monsoon rainfall anomalies, and the role of SST anomalies in the Indian Ocean. *Journal of Geophysical Research: Atmospheres*, **128**, 12, p.e2022JD038112.

Zhang, Z. and Zhou, W., 2021, "Influence of dust aerosols on eastern Pacific tropical cyclone intensity" *Atmospheric and Oceanic Science Letters*, **14**, 3, p.100028.

Zhao, C., Lin, Y., Wu, F., Wang, Y., Li, Z., Rosenfeld, D. and Wang, Y., 2018, "Enlarging rainfall area of tropical cyclones by atmospheric aerosols" *Geophysical Research Letters*, **45**, 16, pp.8604-8611.

Zhao, L., Wang, S.S., Becker, E., Yoon, J.H. and Mukherjee, A., 2020, "Cyclone Fani: the tug-of-war between regional warming and anthropogenic aerosol effects", *Environmental Research Letters*, **15**, 9, p.094020.